

# PEEL STRENGTH TESTING OF FRP APPLIED TO CLAY BRICKS

M. PANIZZA\*, E. GARBIN\* AND M.R. VALLUZZI†

\*University of Padova, Dept. of Civil, Architectural and Environmental Engineering  
Via Marzolo 9, 35131 Padova, Italy  
e-mail: matteo.panizza@unipd.it enrico.garbin@dicea.unipd.it

†University of Padova, Dept. of Cultural Heritage  
Piazza Capitaniato 7, 35139 Padova, Italy  
e-mail: mariarosa.valluzzi@unipd.it

**Key words:** FRP, Masonry, Composites, Peel Strength

**Abstract.** The paper presents a preliminary local investigation related to sliding on a mortar joint due to excessive shear force, mechanism observed during testing of masonry arches and barrel vaults reinforced with Externally Bonded Fibre Reinforced Polymers (EB FRP) at their extrados. This activity was aimed at evaluating a possible contribution of the FRP reinforcement to joint resistance. Fourteen V-shape Peel Tests (VPT) have been performed, which consist in peeling off a central FRP strip from two clay solid bricks aligned along their longitudinal axis, so that the reinforcement assumes a typical “V” shape during detachment. Tests were designed to reproduce and isolate the reinforcement mixed-mode debonding behaviour related to the above mentioned failure mechanism, and their execution allowed assessing experimental setup and procedures.

## 1 INTRODUCTION

Activities herein presented moved from the experimental observation of failure modes of thin masonry barrel vaults and arches strengthened at their extrados by means of Externally Bonded Fibre Reinforced Polymers (EB FRP); in particular, sliding on a mortar joint due to excessive shear force turned out to be a mechanism introduced by the presence of extrados reinforcements [1–4].

The experimentation is based on the idea that FRP strips might offer an additional contribution to joint’s shear resistance of plain masonry, as proposed in [1] and then reported also in [4]. To the purpose of investigating at a local level the behaviour of FRP reinforcements applied to clay substrates and subjected to similar stress conditions, V-shape Peel Tests (VPT) were designed and performed.

Peeling usually indicates the progressive de-

tachment, under external forces, of materials connected by an adhesive layer. In some cases it is supposed that stiffness of one material is sufficiently higher than the other to be considered a rigid material: this is particularly appropriate when dealing with EB FRP applied to concrete or masonry substrates.

Several works refer to the analysis of peeling phenomenon, starting from Bikerman [5], who adopted a peel angle of 90 degrees and identified the failure criterion as maximum elongation of adhesive, evaluated using the theory of beams on elastic soil; its work was reported in [4] as a possible estimation of the FRP contribution to the shear strength of masonry arches with extrados reinforcement.

Gent and Hamed [6] studied the theoretical relation between peel force and peel angle, and compared results of energy-based approach and adhesive stress analysis, imputing differences to

the energy released by local plastic deformations. Nicholson [7] extended results to large deformations and demonstrated the coincidence of the two approaches, in terms of peel force and peel angle relation.

Thouless and Jensen [8] performed an analysis based on linear elastic fracture mechanics of peel test, reported by De Lorenzis and Zavarise [9] who compared analytical formulations to numerical results based on the adoption of uncoupled cohesive interface laws for normal and tangential directions.

Yuan *et al.* [10, 11] proposed an analytical solution for interfacial stresses that affect the interface between FRP laminates and concrete. Sun *et al.* [12] treated analytically and numerically the peel test.

From an experimental point of view, Karbhari *et al.* [13, 14] performed various peel tests on concrete substrates, changing the imposed peel angle. Kimpara *et al.* [15] and Gurgutiutu *et al.* [16, 17] carried out peel tests on the FRP-concrete interface, the first adopting a symmetric set-up while the latter using an asymmetric one. Wan *et al.* [18, 19] adopted a similar asymmetric set-up.

Dai *et al.* [20, 21] carried out experiments to measure mode I, mode II and mixed-mode fracture energies of FRP bonded to concrete, pointing out that fracture energy mode II is not considerably influenced by fibres stiffness, depending firstly on adhesive properties and then on concrete strength, whereas fracture energy mode I depends mainly on substrate properties; concerning mixed-mode fracture energy, the effective length was reported to be rather short and the strength against peel load, whose component orthogonal to the FRP strip was labelled as dowel force, rather low [21].

Other studies by Wu *et al.* [22, 23] on mixed-mode load conditions were performed in Japan, related to application of FRP to intrados of tunnels and bridges as a repair technique aimed at preventing the spalling of deteriorated concrete [24].

Concerning experiments on concrete substrate, it was pointed out [23, 24] that peel force

per unit width and peel angle, during detachment, remain almost constant; it was also observed that peel strength is quite low, and that the presence of a peel force (e.g. at an inclined crack of beams subject to shear and flexure) may affect the global resistance causing a premature detachment of the FRP laminate [24].

## 2 TESTS DESCRIPTION

Aimed at reproducing on the FRP reinforcement a state of stress similar to that related to shear sliding on a mortar joint, a test set-up derived and adapted from those proposed by Wu *et al.* [23] and Dai *et al.* [21] was adopted. In fact, it was estimated more feasible and less problematic, compared to the test method used in a previous activity [25], which revealed some troubles during its execution.

### 2.1 Basic materials

Four sets of solid clay bricks, two extruded (EB1 and EB2) and two facing (FB1 and FB2) brick types, were used as substrate. EB1 and EB2 sets were part of two different batches of extruded bricks type 11010R (produced by Atesina Furnace); FB1 were facing bricks A001GL (Sant’Anselmo Furnace) and FB2 were facing bricks type “*Rosa Vivo*” (San Marco – Terreal Italia). Their measured mechanical properties are listed in Table 1 ( $f_c$ ,  $f_t$ ,  $f_{sp}$  and  $f_{p-o}$  stand for compressive, flexural, splitting and pull-off strength, respectively).

One type of reinforcement system was used, namely high-strength carbon MBrace<sup>®</sup> C1-30; main properties of saturant and fibres are reported in Table 2, as given by producer’s data-sheets.

**Table 1:** Mechanical properties of bricks

Series	$f_c$ N/mm <sup>2</sup>	$f_t$ N/mm <sup>2</sup>	$f_{sp}$ N/mm <sup>2</sup>	$f_{p-o}$ N/mm <sup>2</sup>
EB1	33.3	2.97	1.34	2.75
EB2	38.4	3.89	3.51	3.02
FB1	21.1	5.29	n.a.	1.80
FB2	22.1	5.42	4.02	1.61

**Table 2:** Properties of reinforcement components

Adhesive MBrace <sup>®</sup> Saturant		
Charact. compr. strength	>80	N/mm <sup>2</sup>
Charact. direct tens. strength	>50	N/mm <sup>2</sup>
Maximum tensile strain	2.5	%
Tensile elastic modulus	>3000	N/mm <sup>2</sup>
High-strength Carbon MBrace <sup>®</sup> C1-30		
Equivalent thickness	0.165	mm
Charact. direct tens. strength	3430	N/mm <sup>2</sup>
Maximum tensile strain	1.5	%
Tensile elastic modulus	230000	N/mm <sup>2</sup>

## 2.2 Test setup an procedure

Two solid clay bricks were disposed along their longitudinal axis and bonded to a top steel beam; the beam, sufficiently longer, was provided with two perpendicular steel supports fastened at its ends. They were supported by the rollers of a device used to perform flexural tests.

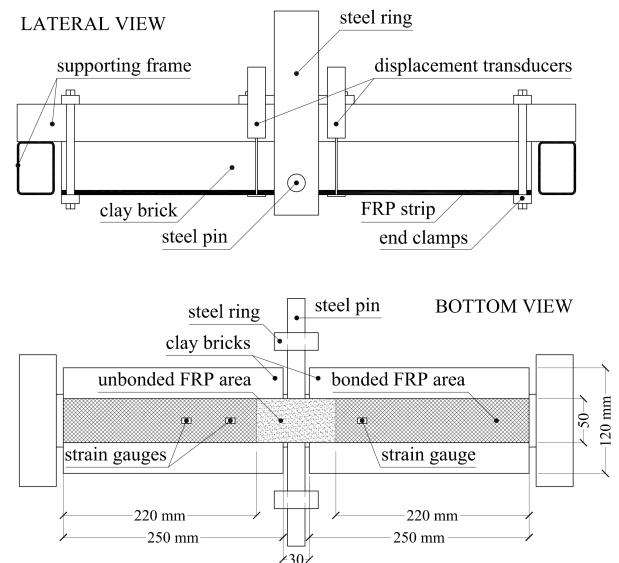
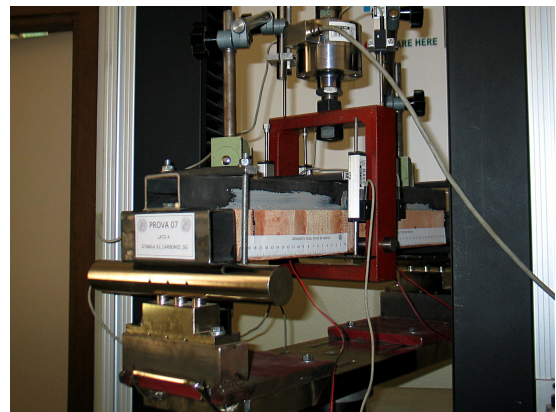
Bricks were fixed only to the top beam, spaced 30 mm apart in order to accommodate the steel pin used to apply the peel force to the reinforcement, and sufficiently spaced from lateral supports to avoid unwanted contacts during test. A reinforcement strip 50 mm wide was applied to the bottom surface of bricks, along their axis; an unbonded area of 30 mm from each brick's central edge was imposed. A detailed scheme is reported in Figure 1, while Figure 2 shows a sample during testing.

Tests were performed on the universal test machine Galdabini SUN2500 (maximum load 25 kN), equipped with an additional load cell connected to the external data acquisition system. The vertical load was transmitted by a solid steel ring surrounding the top beam and connected to a pin acting directly on the FRP strip. Each specimen was monitored by six coupled displacement devices (potentiometers) measuring the lowering in three positions: at the central point, corresponding to the pin, and at the beginning of the bonded areas. Three strain-gauges were applied to the FRP bottom surface of part of the samples.

Loading path, controlled by displacement

rate, was monotonic for five specimens and cyclic for other nine; a pre-loading force of 10 N was applied in order to accommodate part of the deformations related to test system.

The matrix of tests is given in Table 3. Being exploratory tests, some parameters were adjusted during the campaign, as reported in detail in Table 4.

**Figure 1:** Design scheme of a specimen**Figure 2:** Sample ready for test

**Table 3:** Experimental matrix of V-shape Peel Tests

Sample	brick type	loading path
VPT01 (pilot test)	FB2 - facing	monotonic (A)
VPT02 (pilot test)	EB1 - extruded	cyclic (A)
VPT03	EB1 - extruded	cyclic (A)
VPT04	FB2 - facing	cyclic (A)
VPT05	FB2 - facing	monotonic (A)
VPT06	FB2 - facing	cyclic (A)
VPT07	EB1 - extruded	cyclic (B)
VPT08	EB1 - extruded	cyclic (B)
VPT09	EB1 - extruded	monotonic (B)
VPT10	EB1 - extruded	cyclic (B)
VPT11	FB2 - facing	cyclic (B)
VPT12	EB2 - extruded	monotonic (B)
VPT13	FB1 - facing	monotonic (C)
VPT14	FB1 - facing	cyclic (C)

**Table 4:** Adopted test procedures

Procedure	Step	Rate mm/min	Pin direct.	Duration s
Monotonic A	1	2.0	down	up to fail.
	1	2.0	down	180 s
Cyclic A	2	2.0	up	150 s
	3	2.0	down	600 s
	4	back to step 2		
Monotonic B	1	1.0	down	up to fail.
	1	1.0	down	360 s
Cyclic B	2	2.0	up	150 s
	3	2.0	down	600 s
	4	back to step 2		
Monotonic C	1	0.6	down	up to fail.
	1	0.6	down	600 s
Cyclic C	2	1.2	up	250 s
	3	1.2	down	500 s
	4	back to step 2		

## 2.3 Results

An example of typical load – vertical displacement curves for monotonic and cyclic tests are shown in Figure 3. Failure generally involved the detachment of a thin layer of brick, in the case of facing elements (Fig. 5), whereas it was localized at the FRP–substrate interface of extruded bricks, without ripping any clay portion (Fig. 6).

Results, in terms of maximum vertical load  $P_{\max}$  (or dowel load as in [21]), were rather variable, particularly for extruded bricks that showed higher dispersion. Facing bricks generally offered larger values of strength, compared to extruded bricks. This fact could be correlated to the different failure mode observed: facing elements, whose surface is more scabrous and irregular, could have involved a stronger adhesion of the reinforcement, differently from the smoother and more compact extruded bricks.

Table 5 lists maximum loads, together with their corresponding cycle;  $b_f$  is twice the FRP width, while "I" and "S" identify failure localization at the interface or within the substrate, respectively.

Maximum load values were recorded, for all monotonic tests, when reinforcement started to detach from the support; after that peak, vertical loads oscillated within inferior values, however showing a certain scattered trend around a constant or slightly variable value. This trend was slightly different to those observed during cyclic tests, where trends among various peak loads were less recurrent. Concerning cyclic tests, as expected each cycle showed a lower stiffness of the loading/unloading phases, due to the progressive detachment of reinforcement that implied an increasing unbonded length.

However, since load values do not manifest any evident decrease related to the progressive shortening of the bonded area, it could be inferred that effective lengths involved by this mechanism are quite small, possibly about 20–30%, if compared to the effective length related to pure shear debonding. This was previously observed in [21, 23] for concrete specimens and also in [25] for clay bricks.

Monitored displacements allowed to analytically evaluate the slope of reinforcement during detachment, thus the related peel angle  $\theta$ . Figure 4 shows an example of peel angle progression during detachment for both sides of the FRP, and their average measure. Although this estimation was slightly rough, it permitted pointing out some characteristics of the phenomenon.

Facing bricks showed a more scattering evolution of peel angle during the progressive detachment, if compared to extruded bricks; this fact could be justified by the different observed failure mode: detachment involved a thin layer of brittle clay substrate of facing elements, whereas it evolved within the interface or the adhesive in the case of extruded ones.

Measured peel angles for each cycle (or for the whole test in the case of monotonic loading) are reported in Table 6. They mostly ranged from 2 to 6 degrees, values lower than those, about 10 degrees, observed by Wu *et al.* [23] in the case of concrete substrates.  $\theta_{P_{max}}$  correspond to the peak load values, while  $\theta_{avg}$  are average measures during the cycle.

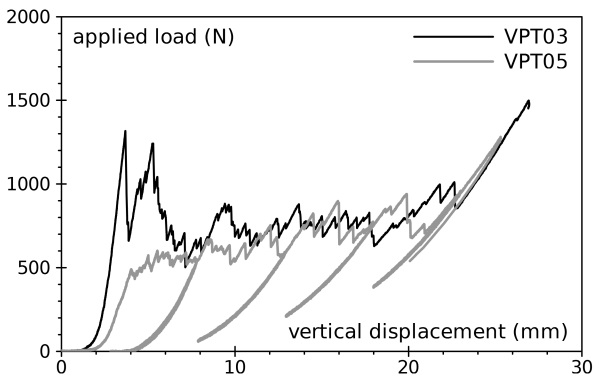


**Figure 3:** Examples of recorded load-displacement functions

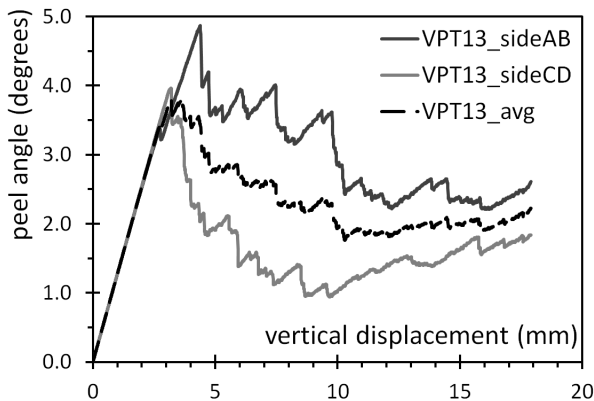


**Figure 4:** Example of peel angle progression



**Figure 5:** Typical failure observed for facing bricks



**Figure 6:** Typical failure observed for extruded bricks

**Table 5:** Experimental results of V-Shape Peel Tests (samples sorted by brick type)

Brick type	Sample	$P_{max}$ N	$P_{max}/b_t$ N/mm	Corresp. cycle	Fail. loc.
EB1	VPT02	1308	13.1	third	I
EB1	VPT03	898	9.0	third	I+S
EB1	VPT07	765	7.7	first	I
EB1	VPT08	850	8.5	second	I
EB1	VPT09	628	6.3	-	I
EB1	VPT10	810	8.1	first	I
EB2	VPT12	940	9.4	-	I
FB1	VPT13	909	9.1	-	S
FB1	VPT14	911	9.1	first	S
FB2	VPT01	1563	15.6	-	S
FB2	VPT04	1283	12.8	second	S
FB2	VPT05	1317	13.2	-	S
FB2	VPT06	1795	18.0	first	I+S
FB2	VPT11	1241	12.4	first	I+S

**Table 6:** Measured peel angles (samples sorted by brick type)

Sample	1 <sup>st</sup> cycle		2 <sup>nd</sup> cycle		3 <sup>rd</sup> cycle	
	$\theta_{P_{\max}}$ deg	$\theta_{\text{avg}}$ deg	$\theta_{P_{\max}}$ deg	$\theta_{\text{avg}}$ deg	$\theta_{P_{\max}}$ deg	$\theta_{\text{avg}}$ deg
VPT02	5.04	5.04	4.20	3.74	4.11	0.75
VPT03	2.87	2.87	n.a.	n.a.	n.a.	n.a.
VPT07	4.31	4.31	3.28	3.02	4.18	3.63
VPT08	5.52	5.52	5.79	4.29	5.04	4.61
VPT09	3.62	3.62				
VPT10	3.08	3.08	2.00	1.97	2.85	2.58
VPT12	5.49	5.49				
VPT13	3.80	3.80				
VPT14	4.58	4.58	3.91	3.68	3.64	3.41
VPT01	4.40	4.38				
VPT04	5.09	5.09	5.10	4.02	n.a.	n.a.
VPT05	3.24	2.92				
VPT06	4.98	4.98	4.13	2.81	2.72	2.44
VPT11	3.77	3.77	3.06	2.41	2.29	1.98

### 3 ANALYSIS OF RESULTS

Based on the evaluated peel angles, and being known the corresponding vertical load, mixed-mode fracture energy components mode I,  $G_I$ , and mode II,  $G_{II}$ , were evaluated following the analysis reported in [9]; total mixed-mode fracture energy  $G$  was assumed to be the sum of its components (see also [13]). Corresponding formulas are reported in Eq. 1–3, where  $E_f$  and  $t_f$  stand for reinforcement elastic modulus and thickness,  $\theta$  is the peel angle and  $F$  the tensile force acting parallel to the FRP. Definition of phase angle  $\psi$  is reported in Eq. 4, together with its practical calculation.

Moreover, the simplified analysis proposed by [23], similarly reported also in [21], was adopted for comparison. Based on simple energy balance considerations, it allows estimating total mixed-mode fracture energy, in this case labelled as  $G_W$ , as a function of vertical dowel load  $P$  and reinforcement axial stiffness per unit width,  $E_f t_f$  (Eq. 5). By re-casting Eq. 5–6, it is possible to estimate the maximum expected dowel load, given a certain fracture energy value (Eq. 7).

Results are listed in Table 7, which compares mixed-mode fracture energies calculated

according to both the cited approaches. It can be noted as they led to very different values, sensibly lower (about 60%) in the second case ( $G_W$ ). Only values related to the maximum recorded load have been reported for each sample.

Phase angles, calculated adopting peak load values, and their corresponding measured peel angles, recorded during each of the first three cycles, or during the whole test in the case of monotonic loading, have been plotted in Figure 7. The chart reports also their analogue average quantities, together with the analytical trend of phase angles evaluated on the basis of the mean dowel load measured for extruded and facing bricks. Related energy components are plotted in Figure 8.

$$F_0 = F \cos \theta \quad (1)$$

$$M_0 = \sqrt{\frac{E_f t_f^3}{6} \left[ \frac{F^2 \sin^2 \theta}{2E_f t_f} + F(1 - \cos \theta) \right]} \quad (2)$$

$$G_I = \frac{6M_0^2}{E_f t_f^3}; \quad G_{II} = \frac{F_0^2}{2E_f t_f}; \quad G = G_I + G_{II} \quad (3)$$

$$\psi = \arctan \sqrt{\frac{G_{II}}{G_I}} = \arctan \frac{t_f F_0}{\sqrt{12} E_f} \quad (4)$$

$$G_W = E_f t_f \left( \frac{1}{2} \tan^2 \theta + \frac{1}{\sqrt{1 + \tan^2 \theta}} - 1 \right) \approx \frac{3}{8} E_f t_f \tan^4 \theta \quad (5)$$

$$P_{\max} = E_f t_f b_f \tan^3 \theta \quad (6)$$

$$P_{\max} = 2.087 b_f G_W^{0.75} (E_f t_f)^{0.25} \quad (7)$$

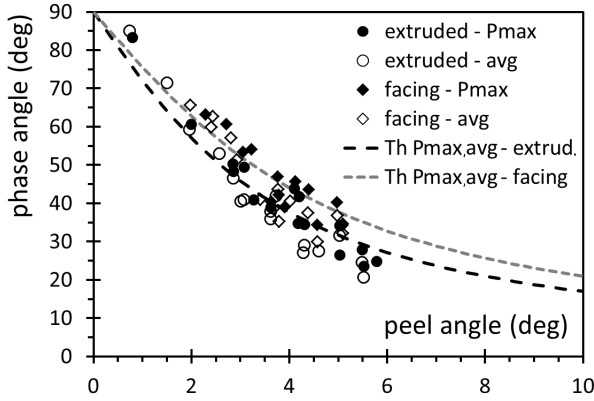


Figure 7: Phase versus peel angles

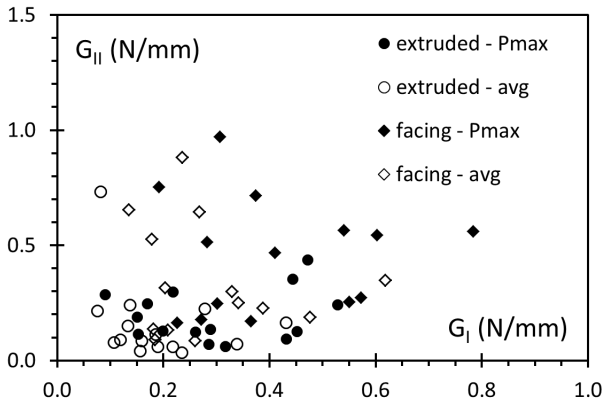


Figure 8: Evaluated mode I and II components of mixed-mode fracture energy

Table 7: Evaluated fracture energies (samples sorted by brick type)

Sample	$G_I$ N/mm	$G_{II}$ N/mm	$\psi$ deg	$G$ N/mm	$G_w$ N/mm	$\Delta G$ %
VPT02	0.472	0.436	43.9	0.908	0.344	-62%
VPT03	0.151	0.190	48.3	0.341	0.122	-64%
VPT07	0.289	0.136	34.4	0.425	0.168	-60%
VPT08	0.431	0.093	24.9	0.524	0.194	-63%
VPT09	0.199	0.129	38.9	0.329	0.129	-61%
VPT10	0.219	0.298	49.4	0.517	0.182	-65%
VPT12	0.452	0.126	27.8	0.578	0.221	-62%
VPT13	0.302	0.247	42.1	0.549	0.212	-61%
VPT14	0.365	0.171	34.4	0.536	0.212	-60%
VPT01	0.603	0.544	43.5	1.147	0.436	-62%
VPT04	0.573	0.273	34.6	0.846	0.335	-60%
VPT05	0.374	0.714	54.1	1.089	0.347	-68%
VPT06	0.784	0.560	40.2	1.344	0.524	-61%
VPT11	0.411	0.467	46.9	0.878	0.321	-63%

## 4 CONCLUSIONS

Fourteen V-shape Peel Tests, which test set-up was based on similar tests carried out on concrete substrates [21, 23], were performed using CFRP reinforcement applied to solid clay bricks. Test were aimed at investigating the possible FRP reinforcement contribution to the shear strength of thin masonry arches and vaults. Although preliminary tests, they allowed identifying the main characteristics of the investigated phenomenon.

The experimental set-up proved to be rather feasible and adaptable to most universal test machines. Observations do not differ much from what Wu *et al.* [23] and Dai *et al.* [21] reported in the case of concrete substrates.

Peel load, during the detachment, oscillated within a limited range, although scattering was in some cases very large; maximum loads of about 8–13 N/mm were observed, except for the FB2 series that resisted up to 18.8 N/mm. First peak load was generally higher than the others, for monotonic tests.

Peel angles, similarly to peel loads, oscillated within a rather moderate range. Measured values varied in most cases between 2 and 6 degrees, however their measurement should be considered qualitative since affected by a certain imprecision and simplifying approximations.

Calculated mixed-mode fracture energies ranged in most cases from 0.3 to 1 N/mm, hence their order of magnitude is rather consistent with values reported in literature for quasi-brittle substrates [9, 21, 23], albeit markedly affected by peel angle measurement.

## 5 ACKNOWLEDGEMENTS

The Authors would like to thank BASF Italy, for having provided the FRP system, and Filippo Giomo, Francesco Balduzzo and Silvia Bordignon for their work. Italian Project ReLUIIS-DPC 2010-2013 and European Project NIKER partially supported the activities.

## REFERENCES

- [1] Valluzzi, M. R., Valdemarca, M. and Modena, C., 2001. Behaviour of brick masonry vaults strengthened by FRP laminates. *ASCE Int. J. of Composites for Construction*. **5**(3):163–169.
- [2] Foraboschi, P., 2004. Strengthening of masonry Arches with Fiber-Reinforced Polymer Strips. *ASCE Int. J. of Composites for Construction*. **8**(3):191–202.
- [3] Basilio, I., 2007. Strengthening of arched masonry structures with composite materials. *Ph.D. Thesis*. University of Minho (Portugal).
- [4] Briccoli Bati, S. and Rovero, L., 2008. Towards a methodology for estimating strength and collapse mechanism in masonry arches strengthened with fibre reinforced polymer applied on external surfaces. *RILEM Materials and Structures*. **41**(7):1291–1306.
- [5] Bikerman, J. J., 1957. Theory of Peeling through a Hookean Solid. *J. of Applied Physics*. **28**(12):1484–1485.
- [6] Gent, A. N. and Hamed, G. R., 1975. Peel Mechanics. *J. of Adhesion*. **7**:91–95.
- [7] Nicholson, D. W., 1977. Peel mechanics with large bending. *Int. J. of Fracture*. **13**(3):279–287.
- [8] Thouless, M. D. and Jensen, H. M., 1992. Elastic Fracture Mechanics of the Peel-Test Geometry. *J. of Adhesion*. **38**:185–197.
- [9] De Lorenzis, L. and Zavarise, G., 2008. Modeling of mixed-mode debonding in the peel test applied to superficial reinforcements. *Int. J. of Solids and Structures*. **45**:5419–5436.
- [10] Yuan, H., Chen, J. F. and Teng, J. G., 2003. Interfacial stresses between FRP plate and concrete in a peel test: an analytical solution. In *Proc. of 10<sup>th</sup> Int. Conf. on Structural Faults + Repair – SF&R2003*. July 1-3, London (UK).
- [11] Yuan, H., Chen, J. F., Teng, J. G. and Lu, X.Z., 2007. Interfacial stress analysis of a thin plate bonded to a rigid substrate and subjected to inclined loading. *Int. J. of Solids and Structures*. **44**:5247–5271.
- [12] Sun, Z., Wan, K. T. and Dillard, D. A., 2004. A theoretical and numerical study of thin film delamination using the pull-off test. *Int. J. of Solids and Structures*. **41**:717–730.
- [13] Karbhari, V. M. and Engineer, M., 1996. Investigation of Bond between Concrete and Composites: Use of a Peel Test. *J. of Reinforced Plastics and Composites*. **15**:208–227.
- [14] Karbhari, V. M., Engineer, M. and Eckel II, D. A., 1997. On the durability of composite rehabilitation schemes for concrete: use of a peel test. *J. of Materials Science*. **32**:147–156.
- [15] Kimpara, I., Kageyama, K., Suzuki, T., Ohsawa, I. and Yamaguchi, K., 1998. Characterization on Peeling Strength of FRP Sheets Bonded on Mortar and Concrete. In *Proc. of 8<sup>th</sup> Japan-U.S. Conf. on Composite Materials*. September 24-25, Baltimore (USA); pp. 1010–1019.
- [16] Giurgiutiu, V., Lyons, J., Petrou, M., Laub, D. and Whitley, S., 1999. Experimental fracture mechanics for the bond between composite overlays and concrete substrate. In *Proc. of Int. Composites Expo – ICE’99*. May 10-13, Cincinnati (USA).
- [17] Giurgiutiu, V., Lyons, J., Petrou, M., Laub, D. and Whitley, S., 2001. Fracture mechanics testing of the bond between composite overlays and a concrete substrate. *J. of Adhesion Science Technology*. **15**(11): 1351–1371.
- [18] Wan, B., Petrou, M. F., Harries, K. A., Sutton, M. A. and Yang, B., 2002. Experimental investigation of bond between FRP and concrete. In *Proc. of 3<sup>th</sup> Int. Conf. on Composites in Infrastructure – ICCI-02*. June 10-13, San Francisco (USA).

- [19] Wan, B., Sutton, M. A., Petrou, M. F., Harries, K. A. and Li, N., 2004. Investigation of Bond between Fiber Reinforced Polymer and Concrete Undergoing Global Mixed Mode I/II Loading. *ASCE Int. J. of Engineering Mechanics* **130**(12):1467–1475.
- [20] Dai, J. and Ueda, T., 2003. Local Bond stress Slip relations for FRP Sheets-Concrete Interfaces. In *Proc. of the 6th Int. Symp. on Fibre-Reinforced Polymer Reinforcement for Concrete Structures – FRPRCS-6*. July 8-10, Singapore (SGP); pp. 143–152.
- [21] Dai, J., Ueda, T. and Sato, Y., 2007. Bonding Characteristics of Fiber-Reinforced Polymer Sheet-Concrete Interfaces under Dowel Load. *ASCE J. of Composites for Construction*. **11**(2):138–148.
- [22] Wu, Z., Yuan, H., Asakura, T., Yoshizawa, H., Kobayashi, A., Kojima, Y. and Ahmed, E., 2005. Peeling Behavior and Spalling Resistance of Bonded Bidirectional Fiber Reinforced Polymer Sheets. *ASCE Int. J. of Composites for Construction*. **9**(3):214–226.
- [23] Wu, Z., Yuan, H., Kojima, Y. and Ahmed, E., 2005. Experimental and analytical studies on peeling and spalling resistance of unidirectional FRP sheets bonded to concrete. *Composites Science and Technology*. **65**:1088–1097.
- [24] Ueda, T. and Dai, J., 2005. Interface bond between FRP sheets and concrete substrates: properties, numerical modelling and roles in member behaviour. *Progress in Structural Engineering Materials*. **7**:27–43.
- [25] Panizza, M., Garbin, E., Valluzzi, M. R. and Modena, C., 2008. Shear Mechanism of Brick Masonry Vaults. In *Proc. of 12<sup>th</sup> Int. Conf. on Structural Faults + Repair – SF&R2008*. June 10-12, Edinburgh (UK).